

Neutron production from the fracture of piezoelectric rocks

This article has been downloaded from IOPscience. Please scroll down to see the full text article.

2013 J. Phys. G: Nucl. Part. Phys. 40 015006

(<http://iopscience.iop.org/0954-3899/40/1/015006>)

View [the table of contents for this issue](#), or go to the [journal homepage](#) for more

Download details:

IP Address: 95.75.206.17

The article was downloaded on 28/12/2012 at 15:52

Please note that [terms and conditions apply](#).

Neutron production from the fracture of piezoelectric rocks

A Widom¹, J Swain¹ and Y N Srivastava²

¹ Physics Department, Northeastern University, Boston MA, USA

² Department of Physics & INFN, University of Perugia, Perugia, Italy

E-mail: John.Swain@cern.ch

Received 2 March 2012

Published 14 December 2012

Online at stacks.iop.org/JPhysG/40/015006

Abstract

A theoretical explanation is provided for the experimental evidence that fracturing piezoelectric rocks produces neutrons. The elastic energy micro-crack production ultimately yields the macroscopic fracture. The mechanical energy is converted by the piezoelectric effect into electric field energy. The electric field energy decays via radio frequency (microwave) electric field oscillations. The radio frequency electric fields accelerate the condensed matter electrons which then collide with protons producing neutrons and neutrinos.

1. Introduction

There has been considerable evidence of high energy particle production during the fracture of certain kinds of crystals [1–6]. In particular, fracture induced nuclear transmutations and the production of neutrons have been clearly observed [7–14]. The production of neutrons appears greatly enhanced if the solids being fractured are piezoelectric [15] materials. Our purpose is to describe theoretically the manner in which the mechanical pressure in a piezoelectric stressed solid about to fracture can organize the energy so that neutrons can be produced.

The nuclear physics involves a standard weak interaction wherein collective radiation plus an electron can be captured by a proton to produce a neutron plus a neutrino

$$\begin{aligned}
 (\gamma + \gamma + \dots + \gamma) + e^- &\equiv \tilde{e}^- \\
 \tilde{e}^- + p^+ &\rightarrow n + \nu_e.
 \end{aligned}
 \tag{1}$$

The symbol \tilde{e}^- represents an electron plus many photons in the initial state. The required collective radiation energy may be produced by the mechanical elastic energy storage via the



Content from this work may be used under the terms of the [Creative Commons Attribution-NonCommercial-ShareAlike 3.0 licence](https://creativecommons.org/licenses/by-nc-sa/3.0/). Any further distribution of this work must maintain attribution to the author(s) and the title of the work, journal citation and DOI.

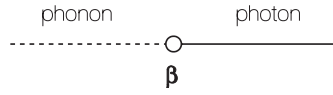


Figure 1. Shown is the Feynman diagram exhibiting the change of a phonon described by the tensor strain w into a photon described by the vector electric field \mathbf{E} and vice versa. The piezoelectric coupling strength tensor $\beta_{i,jk}$ is exhibited in the interaction Hamiltonian equation (3).

piezoelectric effect. By the *definition* of a *piezoelectric material*, the conversions of energy of the form

$$\text{(elastic energy)} \iff \text{(electric energy)} \tag{2}$$

are allowed.

In terms of the electric field \mathbf{E} and the crystal strain tensor w , the precise definition of the piezoelectric tensor β is discussed in section 2. The final result may be expressed as the effective interaction Hamiltonian

$$\mathcal{H}_{\text{int}} = - \int \beta_{i,jk} E_i w_{jk} d^3\mathbf{r}, \tag{3}$$

wherein the tensor coefficients $\beta_{i,jk}$ describe piezoelectricity as shown in figure 1. Some implications of the conversion from mechanical energy into electromagnetic energy are quite striking. For example, a piezoelectric ignition system can be constructed wherein a sharp mechanical impulse to a piezoelectric material can induce a sharp voltage spike across the sample with the resulting spark igniting a fire in a surrounding gas. More dramatically, the rocks crushed in earthquakes contain piezoelectric quartz. The mechanical impulse causing micro-cracks in the rocks can thereby produce impulse earthquake lightning flashes.

In section 3 we discuss the stresses and strains which accompany micro-cracks in rocks that are being fractured. Elasticity theories of such micro-cracks are well known [16–18]. The central result is as follows. If σ_{bond} denotes the elastic stress required to break the chemical bonds on an area of a micro-crack and γ_s denotes the surface tension of the free face of a crack, then the fracture stress σ_F required to create a crack of half length a is given by

$$\sigma_F = \sqrt{\frac{\sigma_{\text{bond}}\gamma_s}{a}} \Rightarrow \sigma_F \ll \sigma_{\text{bond}} \tag{4}$$

for brittle fracture.

In section 4, the manner in which the conversion of mechanical to electrical energy takes place is explored. It is shown that copious electromagnetic energy is emitted in the radio frequency microwave regime. The radiation accelerates the electrons allowing for nuclear transmutations in forms following from the process described through equation (1).

In the concluding section 5, the number of neutrons produced by rock fractures will be estimated.

2. Piezoelectric interactions

The energy per unit volume U of a piezoelectric material obeys

$$dU = TdS + \sigma : dw - \mathbf{P} \cdot d\mathbf{E}, \tag{5}$$

wherein T is the temperature, S is the entropy, σ is the stress tensor, w is the strain tensor, \mathbf{P} is the electric dipole moment per unit volume and \mathbf{E} is the electric field. The adiabatic piezoelectric tensor may be defined as

$$\beta_{i,jk} = \left(\frac{\partial P_i}{\partial w_{jk}} \right)_{S,\mathbf{E}} = - \left(\frac{\partial \sigma_{jk}}{\partial E_i} \right)_{S,w}. \tag{6}$$

To quadratic order, the mechanical electric field interaction energy U_{int} follows from equation (6). It is

$$\begin{aligned}\beta_{i,jk} &= -\frac{\partial^2 U(S, \mathbf{w}, \mathbf{E})}{\partial E_i \partial w_{jk}} = -\frac{\partial^2 U(S, \mathbf{w}, \mathbf{E})}{\partial w_{jk} \partial E_i}, \\ U_{\text{int}} &= -\beta_{i,jk} E_i w_{jk} + \dots,\end{aligned}\quad (7)$$

leading to the quantum operator in the effective Hamiltonian and the Feynman diagram of equation (3).

The adiabatic electric susceptibility of the material at constant strain is defined

$$\chi_{ij} = \left(\frac{\partial P_i}{\partial E_j} \right)_{S, \mathbf{w}}, \quad (8)$$

while the same susceptibility at constant stress is given by

$$\tilde{\chi}_{ij} = \left(\frac{\partial P_i}{\partial E_j} \right)_{S, \sigma}, \quad (9)$$

The elastic response tensor,

$$D_{ijkl} = \left(\frac{\partial w_{ij}}{\partial \sigma_{kl}} \right)_{S, \mathbf{E}}, \quad (10)$$

determines the difference between the two susceptibilities in equations (8) and (9); i.e. the thermodynamic identity is that

$$\tilde{\chi}_{ij} = \chi_{ij} + \beta_{i, lk} D_{lknm} \beta_{j, nm}. \quad (11)$$

For a complex frequency $\zeta = \omega + i\eta$ with $\eta = \Im m \zeta \geq 0$, there are dynamical electric susceptibilities $\tilde{\chi}_{ij}(\zeta)$ and $\chi_{ij}(\zeta)$. The dynamical version of equation (11) is easily obtained. Phonon modes described by the dynamical phonon propagator $D_{lknm}(\zeta)$ affect the dynamical susceptibilities via

$$\begin{aligned}\mathbf{D} &= \mathbf{E} + 4\pi \mathbf{P}, \\ \varepsilon_{ij}(\zeta) &= \delta_{ij} + 4\pi \tilde{\chi}_{ij}(\zeta), \\ \tilde{\chi}_{ij}(\zeta) &= \chi_{ij}(\zeta) + \beta_{i, lk} D_{lknm}(\zeta) \beta_{j, nm}.\end{aligned}\quad (12)$$

Equation (11) is the zero frequency limit $\zeta \rightarrow i0^+$ of equation (12). The dynamical dielectric response tensor $\varepsilon_{ij}(\zeta)$ appears in the polarization part of the photon propagator [19]. The Feynman diagrams contributing to the polarization part of the photon propagator in a piezoelectric system are shown in figure 2. These are equivalent to equation (12) and explain why mechanical acoustic frequencies appear in the electrical response of piezoelectric materials.

3. Fracture and stress

Shown in figure 3 is a crystal under stress σ inducing a micro-crack of width $2a$ and length $L \gg a$. The energy U_b required to create a micro-crack of half width b and length L is given by [17]

$$u(b) = \frac{U_b}{L} = 4\gamma_s b - \pi \left[\frac{(1 - \nu^2)\sigma^2}{\mathcal{E}} \right] b^2, \quad (13)$$

wherein γ_s is the surface tension of the micro-crack interface, \mathcal{E} is the material Young's modulus and ν is the Poisson ratio.

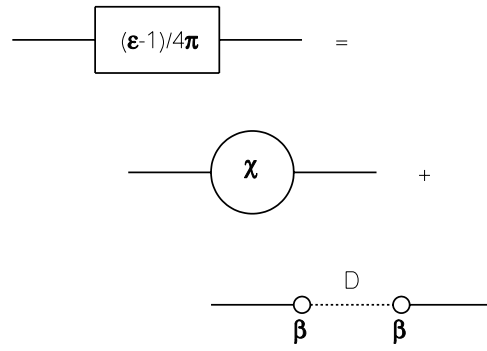


Figure 2. The Feynman diagrams contributing to the polarization part of the photon propagator in a piezoelectric material are shown above. The resulting dielectric response in equations (11) and (12), i.e. $\epsilon_{ij}(\zeta)$, has a contribution due to mechanical phonon modes as exhibited above in diagrammatic form.

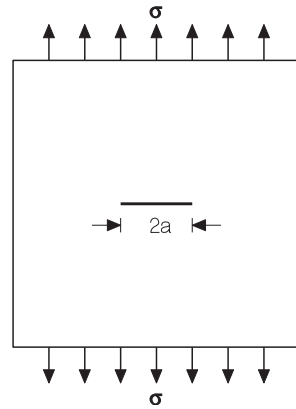


Figure 3. A micro-crack is formed in solid under stress σ . The width of the micro-crack is $2a$ and the length (into the paper) of the crack is $L \gg a$. The half width a is the critical length size for forming the micro-crack as in equation (14).

3.1. Tensile strength

The maximum of the elastic micro-crack energy per unit length ($\max_{b>0} u(b)$) represents the energy barrier to micro-crack creation. In detail,

$$\begin{aligned}
 u &= \max_{b>0} u(b) \text{ at } b = a, \\
 a &= \frac{2\gamma_s}{\pi} \left[\frac{\mathcal{E}}{(1 - \nu^2)\sigma_F^2} \right], \\
 u = 2\gamma_s a &= \frac{4\gamma_s^2}{\pi} \left[\frac{\mathcal{E}}{(1 - \nu^2)\sigma_F^2} \right]. \tag{14}
 \end{aligned}$$

The stress level σ_F which nucleates a micro-crack is thereby the well known result [20]

$$\sigma_F = \sqrt{\frac{2\gamma_s \mathcal{E}}{\pi(1 - \nu^2)a}}. \tag{15}$$

The tensile strength σ_F of the material is then given by equation (4) wherein the broken chemical bond strength

$$\sigma_{\text{bond}} = \frac{2\mathcal{E}}{\pi(1-\nu^2)} \quad (16)$$

is determined by Young's modulus \mathcal{E} and the Poisson ratio ν .

3.2. Numerical estimates

Employing the values of material constants for fused quartz, we can estimate at least the powers of ten that would apply to piezoelectric rocks such as granite rocks. The values are

$$\begin{aligned} \gamma_s &\sim 10^2 \frac{\text{erg}}{\text{cm}^2}, \\ \sigma_{\text{bond}} &\sim 10^{12} \frac{\text{erg}}{\text{cm}^3}, \\ \sigma_F &\sim 10^9 \frac{\text{erg}}{\text{cm}^3}, \\ a &\sim 10^{-4} \text{ cm}, \end{aligned} \quad (17)$$

in satisfactory agreement with the elastic theory as summarized in section 3.1. The chosen value of $\sigma_{\text{bond}} \approx 10^{12} \text{ ergs cm}^{-3}$ corresponds to about $1 \text{ eV } \text{\AA}^{-3}$, a value derived from the theory of breaking chemical bonds. The half length of a micro crack $a \sim 10^{-4} \text{ cm}$ and the surface tension of the free face of a piezoelectric crack $\gamma_s \sim 10^2 \text{ erg cm}^{-2}$ are taken from experiment. Using these values, one can compute σ_F and hence find a posteriori agreement with Griffith's law in the sense that the calculated $\sigma_F \ll \sigma_{\text{bond}}$.

Some comments are in order: (i) For quartz, the value of $a \sim 1$ micron. (ii) For the brittle fracture of quartz, the macroscopic fracture surface experimentally exhibits micro-cracks with a length $L \sim 20$ micron $\gg a$. (iii) As is usual in fractures $\sigma_F \ll \sigma_{\text{bond}}$, i.e. $\sigma_F \sim 10^{-3} \sigma_{\text{bond}}$ for the problem at hand. (iv) The velocity of sound v_s compared with the velocity of light c obeys $(v_s/c) \sim 10^{-5}$. The ratio of phonon frequencies to photon frequencies in cavities of similar length scales thereby obey

$$\left(\frac{\omega_{\text{phonon}}}{\omega_{\text{photon}}} \right) \sim 10^{-5} \quad \text{for similar sized cavities.} \quad (18)$$

The importance of the above equation (18) is that the phonon modes enter into the dynamic dielectric response function $\varepsilon(\omega + i0^+)$ in virtue of equation (12).

4. Neutron production

The neutron production rate at the fracture stress σ_F is here considered due to energetic electrons scattering off protons which are naturally present in (say) granite as water or organic molecules. The Feynman diagram in the Fermi theory limit of the standard model is shown in figure 4 described for the process in equation (1).

4.1. Electron renormalized energy W

To begin to analyze the production of neutrons via the reaction equation (1), one must calculate the mean energy of electrons in condensed matter when accelerated by an electric field

$$\frac{d\mathbf{p}}{dt} = e\mathbf{E}. \quad (19)$$

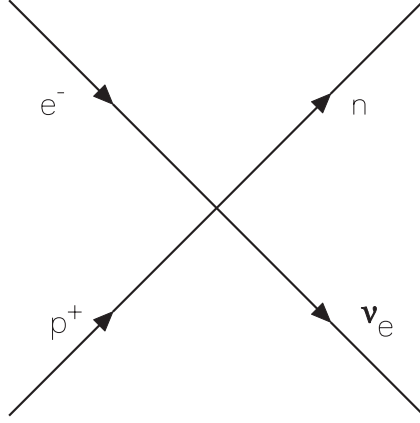


Figure 4. Neutron production takes place via the standard Fermi weak interaction as shown above. The electron energy is renormalized $mc^2 \rightarrow W$ by microwave radiation present as the stress approaches the fracture value σ_F . The coupling strength at the four fermion vertex is G_F .

The electron energy is estimated to be

$$W = \sqrt{m^2c^4 + c^2|\mathbf{p}|^2}. \quad (20)$$

If $P_E(\omega) d\omega$ represents the mean squared electric field strength in a bandwidth $d\omega$, then equation (19), implies

$$E^2 = \int_0^\infty P_E(\omega) d\omega, \quad (21)$$

$$\overline{|\mathbf{p}|^2} = e^2 \int_0^\infty P_E(\omega) \frac{d\omega}{\omega^2}.$$

If Ω denotes the dominant frequency in the spectrum of electric field fluctuations, then equation (21) is more simply written

$$\overline{|\mathbf{p}|^2} = \frac{e^2 E^2}{\Omega^2} \quad (22)$$

so that the ratio of the energy to the rest energy of the electron is

$$\beta = \frac{W}{mc^2} = \sqrt{1 + \left(\frac{eE}{mc\Omega}\right)^2}. \quad (23)$$

The value of $\beta > 1$ is critical for measuring whether or not there is sufficient radiation energy to allow for the reaction in equation (1).

4.2. Further numerical estimates at fracture

To estimate the electric field, one notes that the stress at fracture σ_F is in large part due to the electric field strength

$$\sigma_F \sim \frac{E^2}{4\pi} \Rightarrow E \sim 10^5 \text{ G}, \quad (24)$$

in virtue of equation (17). Since

$$\frac{e}{mc} \approx 1.75882915 \times 10^7 \frac{1}{\text{G s}}, \quad (25)$$

one finds

$$\frac{eE}{mc} \sim \frac{10^{12}}{\text{s}}. \quad (26)$$

The frequency of a sound mode localized on a micro-crack of width $2a$ for a reasonable sound velocity in rock is in the microwave range

$$\Omega \sim \frac{10^{10}}{\text{s}} \quad (27)$$

One should then observe electromagnetic microwave emission when the sound mode is turned into an electromagnetic mode via the piezoelectric effect.

In virtue of equations (23), (26) and (27) one finds $\beta \sim 100$. The threshold value of β for equation (1) to be possible without radiation is $\beta_0 \approx 2.53$ so that the energy renormalized by radiation is above threshold by a wide margin, i.e. $\beta \gg \beta_0$. The electron energies on the surface of a micro-crack in a stressed environment with an external stress σ_F obey

$$W \sim 50 \text{ MeV}. \quad (28)$$

The transition rate per unit time

$$\Gamma(\tilde{e}^- + p^+ \rightarrow n + \nu_e) \approx \left(\frac{G_F m^2}{\hbar c}\right)^2 \left(\frac{mc^2}{\hbar}\right) (\beta - \beta_0)^2, \quad (29)$$

for the process given in equation (1), has been computed [21, 22] as

$$\Gamma(\tilde{e}^- + p^+ \rightarrow n + \nu_e) \approx 10^2 \text{ Hz}. \quad (30)$$

The transition rate per unit time per unit area of micro-crack surfaces may be found from

$$\varpi_2 = n_2 \Gamma(\tilde{e}^- + p^+ \rightarrow n + \nu_e) \quad (31)$$

wherein n_2 is the number of protons per unit micro-crack area in the first few layers of the quartz granite. Typical values are

$$n_2 \sim \frac{10^{13}}{\text{cm}^2} \Rightarrow \varpi_2 \sim 10^{15} \frac{\text{Hz}}{\text{cm}^2}. \quad (32)$$

If the fracture takes place with hydraulic fracture processes, then the neutron production rate will be about a factor of ten higher due to the higher water concentration on the micro-crack surface areas.

5. Conclusions

It is in the nature of piezoelectric matter that strong mechanical disturbances give rise to strong electromagnetic responses. This is true for piezoelectric rocks such as granite which contain large amounts of quartz. For large scale piezoelectric rock fracturing, as takes place in earthquakes, electromagnetic responses in many frequencies, from radio frequency to gamma ray frequency, are to be expected. Some have attributed earthquake lights and/or lightning [23] to the phenomena discussed in this work.

The situation regarding the present theory and experiment for the neutron production from the fracture of piezoelectric rocks is that there is agreement but it is only qualitative. The experimental measurements of emitted neutrons [25] have not yet been calibrated employing a standard neutron source. The output readings of the neutron detections system is far above the background noise and proportional to the neutron production within the crushed rocks. But an absolute measurement of the neutron production rate has not been obtained. Measurements with fully calibrated detection systems represent a central problem for further experiments.

We have employed the standard model of weak interactions along with the known theory of piezoelectric materials to explain the experimental evidence that fracturing piezoelectric rocks produces neutrons. We have also explained why such fracturing processes produce microwave radiation. The elastic energy micro-crack production ultimately yields the macroscopic fracture whose acoustic vibrations are converted into electromagnetic oscillations. The electromagnetic microwaves accelerate the condensed matter electrons which then scatter from protons to produce neutrons and neutrinos. This work also may have implications for a better understanding of radiative processes associated with earthquakes [24, 26].

References

- [1] Karassey V V, Krotova N A and Deryagin B W 1953 *Dokl. Akad. Nauk SSSR* **88** 777
- [2] Klyuev V A, Lipson A G, Toporov Yu P, Deryagin B V, Lushchikov V J, Streikov A V and Shabalin E P 1986 *Sov. Tech. Phys. Lett.* **12** 551
- [3] Klyuev V *et al* 1987 *Kolloidn. Zh.* **88** 1001
- [4] Preparata G 1991 *Il Nuovo Cimento* **104** 1259
- [5] Nakayama K, Suzuki N and Hashimoto H 1992 *J. Phys. D* **25** 303
- [6] Lawn B 1993 *Fracture of Brittle Solids* (Cambridge: Cambridge University Press) 103 section 4.5
- [7] Derjaguin B V, Lipson A G, Kluev V A, Sakov D M and Toporov Yu P 1989 *Nature* **341** 492
- [8] Lipson A G, Sakov D M, Klyuev V A and Deryagin B V 1989 *JETP Lett.* **49** 675
- [9] Derjaguin B V, Kluev V A, Lipson A G and Toporov Y P 1990 *Physica B* **167** 189
- [10] Kaushik T *et al* 1997 *Phys. Lett. A* **232** 384
- [11] Shioe Y *et al* 1999 *Il Nuovo Cimento* **112** 1059
- [12] Cardone F, Carpinteri A and Lacidogna G 2009 *Phys. Lett. A* **373** 862
- [13] Carpinteri A and Lacidogna G 2009 *Strain* **45** 332
- [14] Fuji M *et al* 2002 *Japan. J. Appl. Phys.* **41** 2115
- [15] Landau L D and Lifshitz E M 1984 *Electrodynamics of Continuous Media* (Oxford: Pergamon) section 17
- [16] Freund L B 1998 *Dynamic Fracture Mechanics* (Cambridge: Cambridge University Press)
- [17] Landau L D and Lifshitz E M 1970 *Theory of Elasticity* (Oxford: Pergamon) section 31
- [18] Griffith A A 1921 *Proc. R. Soc.* **221** 161
- [19] Abrikosov A A, Gorkov L P and Dzyaloshinskii I E 1963 *Quantum Field Theory Methods in Statistical Physics* (Englewood Cliffs, NJ: Prentice-Hall) chapter 6
- [20] Landau L D and Lifshitz E M *op. cit.* 146 [17] equation (31.10)
- [21] Widom A and Larsen L 2006 *Eur. Phys. J. C* **46** 107
- [22] Srivastava Y N, Widom A and Larsen L 2010 *Pramana* **75** 617
- [23] Ikeya M and Takaki S 1996 *Japan. J. Appl. Phys.* **35** L355
- [24] Freund F T 2003 Rocks that crackle and sparkle and glow: strange pre-earthquake phenomena *J. Sci Explor.* **17** 37–71
- [25] Carpinteri A, Cardone F and Lacidogna G 2009 *Strain* **45** 332
- [26] Takaki S and Ikeya M 1998 A dark discharge model of earthquake lightning *Japan. J. Appl. Phys.* **37** 5016